Lagrangian Available Energetics and Parcel Instabilities

PETER R. BANNON

Department of Meteorology, The Pennsylvania State University, University Park, Pennsylvania

(Manuscript received 11 September 2003, in final form 16 February 2004)

ABSTRACT

A new derivation of local available energy for a compressible, multicomponent fluid whose base state need not be one of rest that allows for frictional and diabatic processes is presented. The available energy is the sum of the kinetic energy and the available potential and available elastic energies. These energy contributions are defined relative to an arbitrary reference state that can be in motion. Invoking a Lagrangian perspective, it is natural to choose the reference state as the initial state of the parcel. Then the resulting energies are consistent with published formulas for single and binary compressible fluids under inviscid, adiabatic conditions.

When the parcel-theory assumption (that the pressure of the parcel is always that of the environment) is invoked, the available elastic energy is identically zero and a fluid parcel will conserve the sum of its kinetic and available potential energies for inviscid, adiabatic flow. In this case, the parcel's available potential energy is the departure of the parcel's static energy (i.e., the sum of its potential energy and enthalpy) from its initial value. Applications of the theory are made to inertial and symmetric instabilities. Typically the instability is characterized by an increase in kinetic energy at the expense of the available potential energy that becomes negative. In the inertial case, the available potential energy is the negative of the work done by the horizontal pressure gradient force. In the symmetric case, it is the negative of the work done by the horizontal pressure gradient force and the buoyancy force, and it is a modified form of the slantwise convective energy (SCAPE) that includes the work done by the transverse (i.e., perpendicular to the mean flow) Coriolis forces. A convenient method to determine the longitudinal (i.e., parallel to the mean flow) and transverse contributions to the kinetic energy is presented. For upright convection, the decrease in the parcel's available potential energy equals its convective available potential energy. Comparison to traditional energetics is made.

1. Introduction

Margules (1905) articulated the observation that, of the large reservoirs of internal and potential energies in the atmosphere, only a small portion is transformed into the kinetic energy of atmospheric motions. Thus, only part of the energy reservoir is available for transformation. Building on this idea, Lorenz (1955) introduced the concept of available potential energy as the maximum kinetic energy attainable by an adiabatic redistribution of the mass of a hydrostatic atmosphere. He formulated a global theory of available potential energy that has become a cornerstone for describing the general circulation of the atmosphere. Lorenz (1955, p. 158) noted that ''the available potential energy is positive if the stratification is not both horizontal and statically stable.'' Margules also discussed the energy attainable from statically unstable conditions. This energy is often referred to as convective available potential energy (CAPE).

Andrews (1981) advanced the theory of available potential energy to include an available elastic energy for compressible nonhydrostatic flows. The positive definite form of the available energies was emphasized for stably stratified flows. Shepherd (1993) presented a unified theory of available energetics that embraces the formalism of Hamiltonian dynamics. Bannon (2003) utilized this formalism to extend the theory to binary fluids. Here, binary refers to the presence of two components of the fluid, such as solids dissolved in a liquid or gaseous and liquid water existing along with dry air.

The purpose of this paper is to present (in section 2) a simple, but general, derivation of the available energetics for a compressible, multicomponent fluid that utilizes a Lagrangian perspective. It is then noted that the available energetics takes on a particularly simple and useful form when the parcel theory assumption is made that the perturbation pressure vanishes. Then, the available elastic energy vanishes, the available potential energy is the change in the parcel's static energy, and the sum of the kinetic and available potential energies is conserved for adiabatic inviscid flow. Sections 3 and 4 apply these parcel results to examine the available and traditional energetics of inertial and symmetric instabilities. The inertial cases cover the stable, neutral, and unstable cases, as well as a case of nonlinear instability.

Corresponding author address: Peter R. Bannon, Dept. of Meteorology, The Pennsylvania State University, University Park, PA 16802.
E-mail: bannon@ems.psu.edu

Inertial instability is believed to be important in limiting the anticyclonic shear of the jet stream (e.g., Holton 1992, p. 208). The symmetric cases extend the nonhydrostatic and hydrostatic Boussinesq analysis of Emanuel (1983a). Cases of closed and pseudoadiabatic conditional symmetric instabilities with phase changes are also examined. Symmetric instability is believed to be important in the formation of frontal rainbands (e.g., Holton 1992, p. 277). These analyses help unify the relations of available potential energy, CAPE, and slantwise convective available potential energy (SCAPE; Emanuel 1983b). Section 5 summarizes the results and presents a refinement of the theory.

2. A general derivation of Lagrangian available energetics

This section presents a simple derivation of the general result for the available energy for a compressible, multicomponent, single-velocity fluid. The specific kinetic energy ke $= |\mathbf{u}|^2/2$ equation may be written as

$$\frac{\partial \mathrm{ke}}{\partial \tau} \equiv \frac{\partial}{\partial \tau}\left(\frac{\mathbf{u}\cdot\mathbf{u}}{2}\right) = -\frac{1}{\rho_p}\mathbf{u}\cdot\nabla p - \mathbf{u}\cdot\nabla\Phi + \mathbf{u}\cdot\mathbf{f}, \tag{2.1}$$

where $\mathbf{u}$ is the three-dimensional velocity field, ρ_p is the parcel's density, p is the pressure, Φ is the geopotential, $\mathbf{f}$ is the specific frictional force, and $\partial/\partial\tau$ is the Lagrangian rate of change with time τ. Here and elsewhere, lowercase symbols are used for the energy terms and the frictional force because they are specific energies and forces. The specific potential energy pe equation is

$$\frac{\partial \mathrm{pe}}{\partial \tau} = \mathbf{u}\cdot\nabla\Phi, \tag{2.2}$$

and the potential energy increases during ascent when work is being done against gravity. For a Cartesian geometry pe $= gz$, where g is the acceleration due to gravity and z is a vertical displacement. Adding the kinetic energy equation to this last result yields the mechanical energy equation

$$\begin{aligned}\frac{\partial(\mathrm{ke}+\mathrm{pe})}{\partial\tau} &= -\frac{1}{\rho_p}\mathbf{u}\cdot\nabla p + \mathbf{u}\cdot\mathbf{f}\\ &= -\frac{1}{\rho_p}\mathbf{u}\cdot\nabla p' - \frac{1}{\rho_p}\mathbf{u}\cdot\nabla p_s + \mathbf{u}\cdot\mathbf{f}\\ &= -\frac{1}{\rho_p}\nabla\cdot(p'\mathbf{u}) + \frac{1}{\rho_p}p'\nabla\cdot\mathbf{u}\\ &\quad - \frac{1}{\rho_p}\mathbf{u}\cdot\nabla p_s + \mathbf{u}\cdot\mathbf{f},\end{aligned} \tag{2.3}$$

where the pressure is divided into a base state p_s and perturbation component p'. The base state is taken to be a balanced initial configuration (e.g., in geostrophic and hydrostatic balance). The specific enthalpy k equation is

$$\begin{aligned}\frac{\partial k}{\partial\tau} &= \frac{1}{\rho_p}\frac{\partial p}{\partial\tau} + \dot{q}\\ &= \frac{1}{\rho_p}\frac{\partial p'}{\partial\tau} + \frac{1}{\rho_p}\frac{\partial p_s}{\partial\tau} + \dot{q}\\ &= \frac{1}{\rho_p}\frac{\partial p'}{\partial\tau} + \frac{1}{\rho_p}\mathbf{u}\cdot\nabla p_s + \dot{q},\end{aligned} \tag{2.4}$$

where $\dot{q}$ represents the diabatic processes (i.e., radiation conduction, and viscous dissipation). Definitions of the enthalpy for a dry and moist fluid parcel are given in sections 3 and 4. No terms for chemical and/or phase changes appear explicitly in (2.4) because their effects are contained implicitly in the multicomponent enthalpy term on the left-hand side of the equation. The last equality in (2.4) follows from the assumption that the base-state pressure is not a function of time. Adding this to our mechanical energy equation yields

$$\begin{aligned}\frac{\partial(\mathrm{ke}+\mathrm{pe}+k)}{\partial\tau} &= -\frac{1}{\rho_p}\nabla\cdot(p'\mathbf{u}) + \frac{1}{\rho_p}p'\nabla\cdot\mathbf{u}\\ &\quad + \frac{1}{\rho_p}\frac{\partial p'}{\partial\tau} + \mathbf{u}\cdot\mathbf{f} + \dot{q}.\end{aligned} \tag{2.5}$$

Using the continuity equation for the divergence term on the right-hand side yields

$$\frac{1}{\rho_p}p'\nabla\cdot\mathbf{u} + \frac{1}{\rho_p}\frac{\partial p'}{\partial\tau} = -\frac{1}{\rho_p^2}p'\frac{\partial\rho_p}{\partial\tau} + \frac{1}{\rho_p}\frac{\partial p'}{\partial\tau} = \frac{\partial}{\partial\tau}\left(\frac{p'}{\rho_p}\right). \tag{2.6}$$

Then (2.5) may be written as

$$\frac{\partial}{\partial\tau}\left(\mathrm{ke}+\mathrm{pe}+k-\frac{p'}{\rho_p}\right) = -\frac{1}{\rho_p}\nabla\cdot(p'\mathbf{u}) + \dot{q} + \mathbf{u}\cdot\mathbf{f}, \tag{2.7}$$

which is a convenient form of the energy equation. At this juncture, the potential energy and the enthalpy are defined relative to a reference value

$$\mathrm{pe} = \mathrm{pe}_0 + \mathrm{pe}', \qquad k = k_0 + k', \tag{2.8}$$

where the reference value, denoted by a subscript zero, may be defined for each parcel. Although the choice of the reference value is arbitrary, it is natural in a Lagrangian formulation to define it in terms of the initial configuration of the parcel:

$$\mathrm{pe}_0 = \mathrm{pe}_i, \qquad k_0 = k_i, \tag{2.9}$$

indicated by the subscript i. [In analogy with (2.8) and (2.9), one could also define ke $=$ ke$_i$ + ke$'$, where ke$_i$ is, say, the kinetic energy of the initial perturbation. However, this kinetic energy departure could then be-

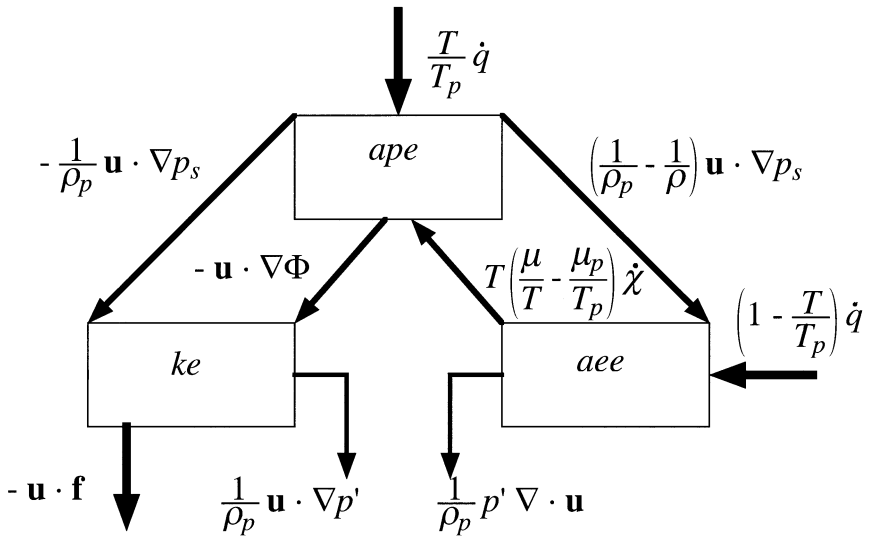

FIG. 1. Schematic diagram of the Lagrangian available energetics for a binary fluid. The relationship between the specific available elastic (aee), available potential (ape), and kinetic energy (ke) are shown with thick arrows indicating generation processes and thin arrows indicating conversion mechanisms. The direction of the arrows indicates the direction of positive energy transfer.

come negative. To avoid this situation and without loss of generality, the choice $\mathrm{ke}_0 = 0$ is made even though the parcel may have kinetic energy initially.] Then the Lagrangian form for the available energy equation is

$$\frac{\partial \mathrm{ae}}{\partial \tau} = -\frac{1}{\rho_p}\boldsymbol{\nabla}\cdot(p'\mathbf{u}) + \dot{q} + \mathbf{u}\cdot\mathbf{f}, \qquad (2.10)$$

where the specific available energy ae is

$$\mathrm{ae} = \mathrm{ke} + \mathrm{pe}' + k' - \frac{p'}{\rho_p}. \qquad (2.11)$$

It is important to note that the available energy of the parcel is conserved for inviscid, adiabatic flow with no pressure perturbation. In addition, the global mass-integrated available energy will be conserved in inviscid, adiabatic flow in a fixed, closed domain. Lastly, the form of (2.10) is consistent with that of Andrews (1981) for an inviscid, adiabatic, single-component fluid.

Generalizing the results of Andrews (1981) and Bannon (2003) to a multicomponent fluid, the specific available elastic energy is defined as

$$\mathrm{aee} = k(p_p, \eta_p, \boldsymbol{\chi}_p) - k(p_s, \eta_p, \boldsymbol{\chi}_p) - \frac{p'}{\rho_p}, \qquad (2.12)$$

where η is the entropy and $\boldsymbol{\chi} = (\chi_1, \chi_2, \ldots \chi_N)$ is the concentration vector for the N constituents where χ_j is the concentration of the jth constituent. This elastic energy represents the change in the compressional potential energy associated with the perturbation pressure p'. Then the available potential energy is

$$\mathrm{ape} = \mathrm{pe}' + k(p_s, \eta_p, \boldsymbol{\chi}_p) - k(p_i, \eta_{pi}, \boldsymbol{\chi}_{pi}), \qquad (2.13)$$

and the available energy is the sum of the kinetic, available potential, and available elastic energies

$$\mathrm{ae} = \mathrm{ke} + \mathrm{ape} + \mathrm{aee}. \qquad (2.14)$$

The results (2.10)–(2.14) for viscous, diabatic flow are consistent with the analyses of Andrews (1981), Shepherd (1993), and Bannon (2003) for inviscid, adiabatic flow. This completes the derivation.

The individual components of the available energetics are summarized in Fig. 1 based on the following equations:

$$\frac{\partial \mathrm{ke}}{\partial \tau} = -\frac{1}{\rho_p}\mathbf{u}\cdot\boldsymbol{\nabla}p_s - \frac{1}{\rho_p}\mathbf{u}\cdot\boldsymbol{\nabla}p' - \mathbf{u}\cdot\boldsymbol{\nabla}\Phi + \mathbf{u}\cdot\mathbf{f}, \qquad (2.15a)$$

$$\frac{\partial \mathrm{ape}}{\partial \tau} = \mathbf{u}\cdot\boldsymbol{\nabla}\Phi + \frac{1}{\rho_p}\mathbf{u}\cdot\boldsymbol{\nabla}p_s + \left(\frac{1}{\rho}-\frac{1}{\rho_p}\right)\mathbf{u}\cdot\boldsymbol{\nabla}p_s + \frac{T}{T_p}\dot{q} + T\left(\frac{\mu}{T}-\frac{\mu_p}{T_p}\right)\dot{\chi}, \qquad (2.15b)$$

$$\frac{\partial \mathrm{aee}}{\partial \tau} = -\frac{1}{\rho_p}p'\boldsymbol{\nabla}\cdot\mathbf{u} + \left(\frac{1}{\rho_p}-\frac{1}{\rho}\right)\mathbf{u}\cdot\boldsymbol{\nabla}p_s + \left(1-\frac{T}{T_p}\right)\dot{q} - T\left(\frac{\mu}{T}-\frac{\mu_p}{T_p}\right)\dot{\chi}, \qquad (2.15c)$$

that sum to give (2.10). For simplicity, the equations for a binary (i.e., two component) fluid are presented. Here $\dot{\chi}$ is the rate of change of the concentration of the minor constituent with concentration χ and chemical

potential μ relative to the major constituent. The multicomponent case is a straightforward extension. Here, ρ, μ, and T are functions of p_s, η_p, and χ_p, and they represent the density, chemical potential, and temperature of the parcel if it were at the pressure of the base state at its location. Note that the available elastic energy and all of its source terms on the right-hand side of (2.15c) depend upon the difference between the pressure of the parcel and that of its environment, and thus they vanish when that difference vanishes.

Next, these available results are compared with those for traditional energetics for which the energy equation is

$$\frac{\partial \text{te}}{\partial \tau} = -\frac{1}{\rho_p}\nabla \cdot (p\mathbf{u}) + \mu_{pj}\dot{\chi}_j + \dot{q} + \mathbf{u} \cdot \mathbf{f}, \quad (2.16)$$

where the total/traditional energy te is defined relative to its initial value as

$$\text{te} = \text{ke} + \text{pe}' + \text{ie}'. \quad (2.17)$$

Here, ie is the specific internal energy. Henceforth, the primes in (2.17) are dropped. Comparison of (2.16) with (2.10) indicates that the available energy as defined in this formulation has subsumed the contribution of the rate of working by the base-state pressure field into the available energy. Here, the rate of working $-\nabla \cdot (p\mathbf{u})$ by the pressure field is the sum of the rate of the work done by the pressure gradient force and the rate of work done by the pressure field in compressing the fluid parcel.

To apply this analysis to the case of parcel theory, the base state is taken to be that of the environment. Then the perturbation pressure p', the available elastic energy, and the rate of working by the perturbation pressure vanish. Thus, the available energetics simplifies considerably and the available potential energy is the difference in the parcel's static energy h from its initial static energy

$$\text{ape} = h_p - h_i, \quad (2.18)$$

where $h = k + gz$. Then, for a closed, inviscid, adiabatic system (2.10) becomes

$$\frac{\partial \text{ae}}{\partial \tau} = 0, \quad (2.19)$$

where

$$\text{ae} = \text{ke} + \text{ape}.$$

The result (2.19) has been used by several investigators in various forms. Peslin (1868) applied it to cumulonimbus energetics as CAPE (see also Madden and Robitaille 1970). Margules (1905) applied it to a buoyancy oscillation. Danielsen (1961) applied it to help construct synoptic-scale trajectories. Green et al. (1966; see also Betts and McIlveen 1969) extended the application to the three-dimensional trajectories of trade wind air ascending into the jet stream.

In the next two sections, the result (2.19) is applied to four cases of inertial oscillations and instabilities (section 3) and to four cases of moist and dry symmetric instabilities (section 4). In all cases, the base state is not one of rest. The relationship of compressible available energetics to the Boussinesq SCAPE of Emanuel (1983b) is clarified (cf. Gray and Thorpe 2000).

3. Inertial flows

a. Base state

Consider a dry, ideal gas in hydrostatic and geostrophic balance on an f plane. The temperature of the environment is given by

$$T_e(x, z) = T_0 - \Gamma z + \alpha x + \frac{\beta x^2}{2} + \frac{\gamma x^3}{3}, \quad (3.1)$$

where T_0 is a constant reference temperature and Γ is the lapse rate. The parameters α, β, and γ describe the horizontal variation of the temperature field. They are chosen to describe flows of various structures. In order to isolate purely inertial flows, the buoyancy force is suppressed by assuming a dry, isentropic, base state whose potential temperature is a constant $\theta_e = T_0$. Then, the lapse rate is the dry adiabatic lapse rate $\Gamma = g/c_p$, where g is the acceleration due to gravity and c_p is the specific heat at constant pressure. An adiabatic lapse rate is typical of the atmospheric boundary layer. The pressure and density fields are

$$p_e = p_{00}\left(\frac{T_e}{T_0}\right)^{c_p/R}, \qquad \rho_e = \frac{p_e}{RT_e}, \quad (3.2)$$

where p_{00} is the constant pressure used to define the potential temperature, and R is the gas constant for dry air. The horizontal pressure gradients support a geostrophic mean wind of the form

$$v_e \equiv \frac{1}{\rho_e f}\frac{\partial p_e}{\partial x} = \frac{c_p}{f}(\alpha + \beta x + \gamma x^2), \quad (3.3)$$

which is independent of height. The pseudoabsolute momentum of the environment is

$$M_e \equiv v_e + fx. \quad (3.4)$$

b. Parcel dynamics

We assume inviscid, adiabatic, parcel dynamics and examine the parcel's motion and available energetics in four different environmental flows corresponding to inertially stable, unstable, neutral, and nonlinearly unstable configurations. In each case, the parcel initially lies at the origin and at the initial time is given a transverse [i.e., perpendicular to the mean flow (3.3)] velocity perturbation of $u_i = -20$ m s^{-1}. Because the flow is adiabatic, the parcel conserves its potential temperature. By the assumption of parcel theory, its pressure is always

that of the environment. Thus, the parcel's temperature and density is always that of its surroundings and the buoyancy force is identically zero. This result and the fact that the initial perturbation is horizontal ensure that the parcel remains in the horizontal plane. The Lagrangian equations of motion for the parcel are

$$\frac{\partial u_p}{\partial \tau} = -\frac{1}{\rho_p}\frac{\partial p_e}{\partial x} + f v_p = f(v_p - v_e), \quad (3.5a)$$

$$\frac{\partial v_p}{\partial \tau} = -f u_p, \quad (3.5b)$$

$$\frac{\partial \theta_p}{\partial \tau} = 0, \quad (3.5c)$$

and the parcel trajectory is given by

$$\frac{\partial x_p}{\partial \tau} = u_p, \qquad \frac{\partial y_p}{\partial \tau} = v_p. \quad (3.6)$$

The longitudinal (i.e., parallel to the mean flow) momentum equation (3.5b) implies the parcel conserves its pseudoabsolute momentum $M_p = v_p + f x_p$. Then the transverse acceleration (3.5a) may be written in terms of the pseudomomenta of the parcel and the environment as

$$\frac{\partial u_p}{\partial \tau} = M_p - M_e. \quad (3.7)$$

This nonlinear set of coupled equations may be solved numerically using a standard Runge–Kutta technique.

c. Four cases of inertial flow

The first three cases consider a linear shear flow, and the temperature parameters α, β, and γ are such that $v_e = \zeta_e x$, where ζ_e is the uniform environmental relative vorticity. Linear theory (e.g., Dutton 1995, section 9.4) predicts the parcel is stable, unstable, or neutral if the absolute vorticity $f + \zeta_e$ is positive, negative, or zero. Each case is examined in turn.

Figure 2 presents the numerical results for the stable case of the relative vorticity equal to f. Consistent with analytic theory (van Mieghem 1951), the parcel's trajectory (Fig. 2b) is that of an ellipse

$$x_p = -\frac{u_0}{\omega}\sin\omega\tau, \qquad y_p = \frac{f u_0}{\omega^2}(1 - \cos\omega\tau), \quad (3.8)$$

centered at $(x = 0, y = -f u_0/\omega^2)$, where $\omega^2 = f(f + \zeta_e)$ and $u_0 = 20$ m s^{-1}. The period of the inertial oscillation is 12.34 h.

Figure 2c demonstrates that the parcel conserves the sum of its kinetic and available potential energies. Here, the parcel's potential energy is a constant, and its available potential energy is the departure of its enthalpy from its initial value ape $= c_p(T - T_0)$. The available energetics is readily understood by noting that the pressure field is a minimum at the origin (Fig. 2a). Just after the initial time, the parcel is moving westward against

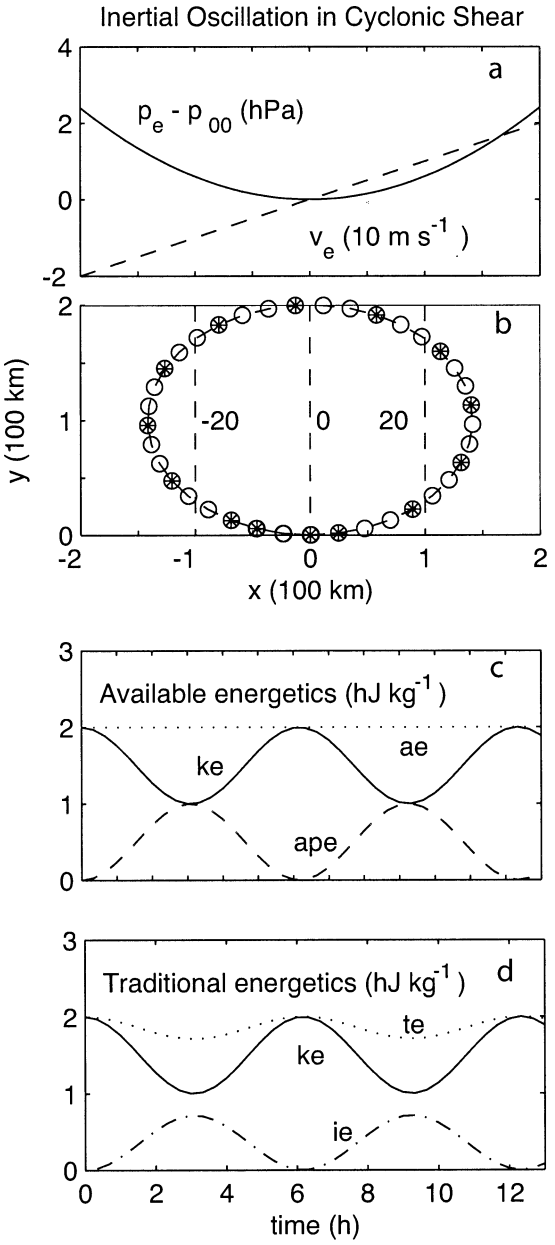

FIG. 2. (a) Environmental pressure and longitudinal wind as a function of transverse distance x, (b) parcel trajectory, and (c) available and (d) traditional energetics as a function of time for the case of a stable inertial oscillation with $\zeta_e = f$. In (a), the pressure departure from the origin (in hPa) and the longitudinal wind (in 10 m s^{-1}) are indicated by the solid and dashed curves. In (b), the parcel location is indicated with an open circle every 20 min and with an asterisk every hour. The parcel is initially at the origin and moves anticyclonically. The dashed lines in (b) are contours of the environmental pseudoabsolute momentum with contour interval of 20 m s^{-1}. In (c), the kinetic and available potential energies are indicated as solid and dashed curves. Their sum, the available energy ae indicated by the dotted curve, is a constant. In (d) the kinetic, internal, and total energies are indicated by the solid, dashed, and dotted curves.

the ambient pressure gradient force, and its kinetic energy is decreasing. At the same time, the parcel is experiencing higher pressures that squeeze the parcel, reducing its volume and increasing its temperature. The change in kinetic energy is balanced by a change in the available potential energy so that their sum is conserved. Mathematically, one finds

$$\frac{\partial \text{ke}}{\partial \tau} = -\frac{u_p}{\rho_p}\frac{dp_e}{dx}, \qquad \frac{\partial \text{ape}}{\partial \tau} = \frac{u_p}{\rho_p}\frac{dp_e}{dx}. \tag{3.9}$$

Figure 2c demonstrates that both energies are positive in this stable case and they oscillate at a frequency twice that of the trajectory. The fact that they take on the same value partway through the oscillation is fortuitous in this case. For example, for the oscillation in the absence of shear, the kinetic energy is constant, and the available potential energy vanishes; for the case of a larger cyclonic shear, the available potential energy can exceed the kinetic energy.

An inertial available potential energy

$$\text{IAPE} \equiv -\int_{\tau_i}^{\tau_f} \frac{u_p}{\rho_p}\frac{dp_e}{dx}\,d\tau = \text{ape}(\tau_i) - \text{ape}(\tau_f) \tag{3.10}$$

is the change in the kinetic energy due to the work done by the pressure gradient force from some initial to some final time following the parcel. The second equality follows from the second equality in (3.9) and states that the IAPE is just the difference in the parcel's enthalpy at the two times. In contrast to the definition (3.10), Rauber et al. (1994) defined IAPE as the longitudinal kinetic energy associated with slantwise available potential energy.

Figure 2d demonstrates the efficacy of the available energetics description of Fig. 2c by plotting the terms in the traditional energetics. In this approach, the parcel does not conserve its total energy. Rather, there is an exchange of energy with the environment associated with the rate of working term in (2.16) by the environmental pressure.

Figure 3 presents the numerical results for the unstable case of the relative vorticity equal to $-2f$. Consistent with analytic theory, the parcel's trajectory (Fig. 3b) is that of a hyperbola

$$x_p = -\frac{u_0}{\sigma}\sinh\sigma\tau, \qquad y_p = -\frac{fu_0}{\sigma^2}(1 - \cosh\sigma\tau), \tag{3.11}$$

centered at $(x = 0, y = 0)$, where $\sigma^2 = -f(f + \zeta_e)$. The available energetics (Fig. 3c) is again understood by noting that the pressure field (Fig. 3a) is a maximum at the origin. Just after the initial time the parcel is moving westward down the ambient pressure gradient, and its kinetic energy is increasing. At the same time, the parcel is experiencing lower pressures (Figs. 3a,b), and the parcel expands and cools. The change in kinetic energy is balanced by a change in the available potential energy so that their sum is conserved. However, unlike the stable case, the available potential energy is increasingly negative. The amplitudes of both energies grow exponentially with time. In the traditional energetics (Fig. 3d), the increase in the kinetic energy dominates the decrease in internal energy, and the total energy increases, implying that the environment is doing work on the parcel.

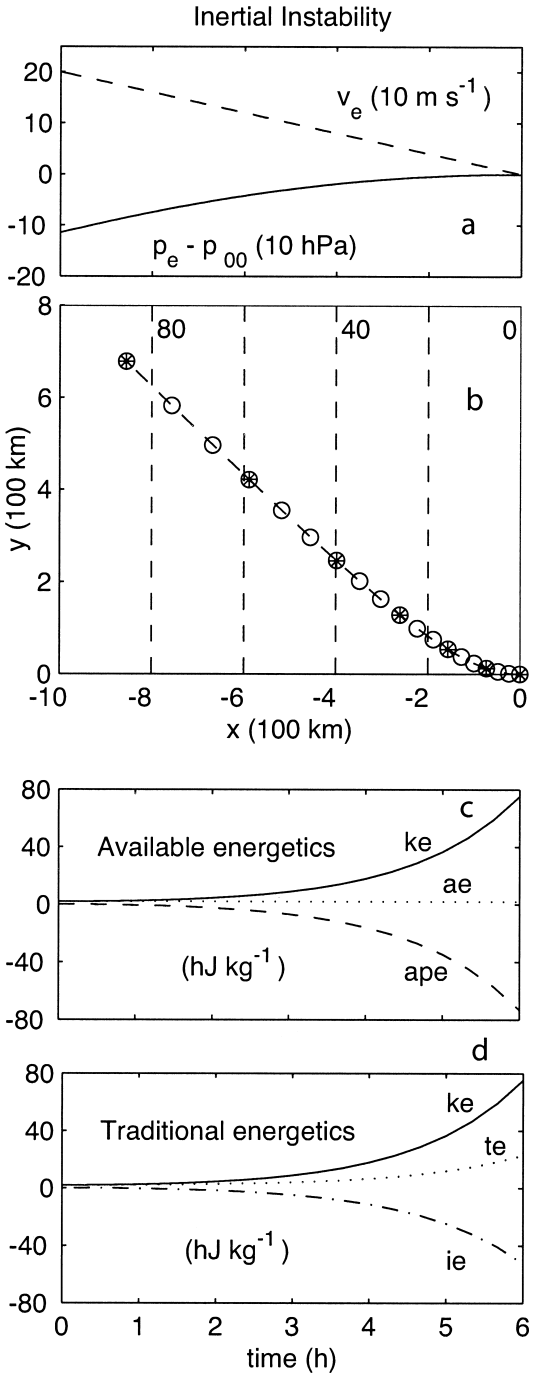

FIG. 3. As in Fig. 2, for the case of an unstable inertial flow with $\zeta_e = -2f$. In (a), the pressure departure from the origin (in 10 hPa) and the longitudinal wind (in 10 m s^{-1}) are indicated by the solid and dashed curves.

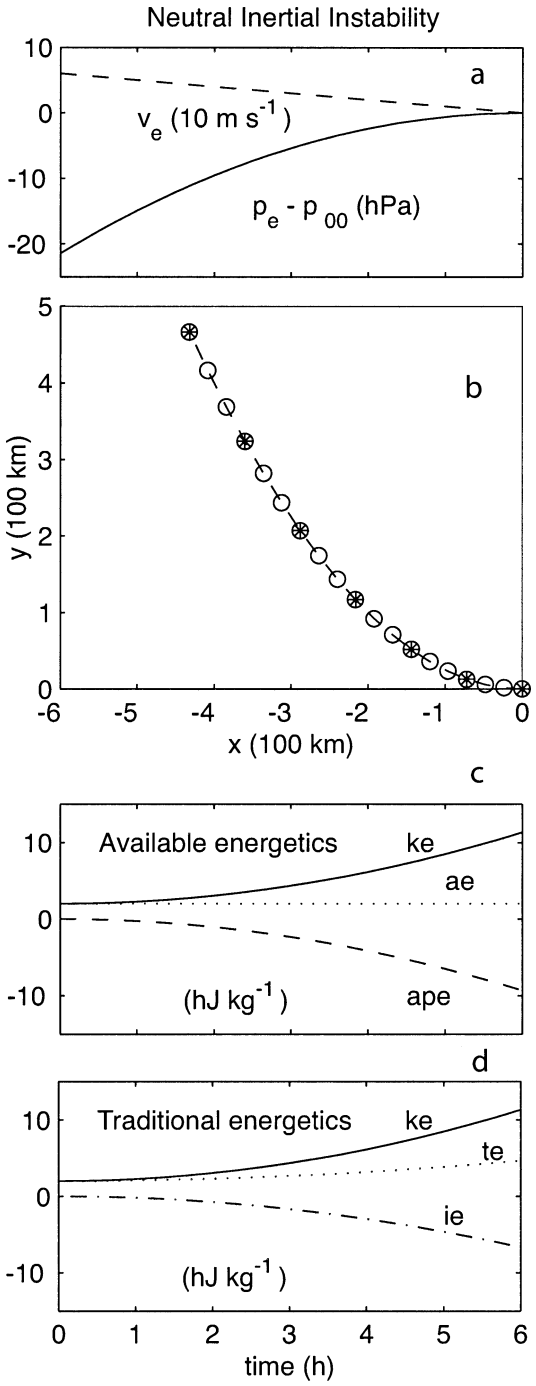

FIG. 4. As in Fig. 2, but for the case of a neutral inertial flow with $\zeta_e = -f$.

The third case is predicted to be neutral in linear theory but is actually unstable in nonlinear theory (e.g., Dutton 1995, section 9.4). When $\zeta_e = -f$, the trajectory (Fig. 4) is a parabola

$$x_p = -u_0\tau, \qquad y_p = \frac{fu_0\tau^2}{2}. \tag{3.12}$$

Unlike the exponential growth of the kinetic energy in the unstable case, the growth in the ''neutral'' case (Fig. 4) is similar to that of Fig. 3, but is quadratic in time. Again, the available energy is conserved.

The fourth and final inertial case (Fig. 5) is one of nonlinear instability. The thermal parameters α, β, and γ are chosen to produce a longitudinal jet (Fig. 5a) of the form

$$v_e = v_0(1 - x^2/a^2), \tag{3.13}$$

where $v_0 = 20$ m s^{-1} and $a = 200$ km. Then the absolute vorticity is positive for $x < 100$ km, vanishes at $x = 100$ km, and is negative for $x > 100$ km. According to (3.7), a parcel at the origin with $M_p = 20$ m s^{-1} must be displaced more than 200 km eastward to encounter M_e values less than this value and be unstable. Because its initial velocity perturbation is westward, the parcel takes about 10 h to traverse this distance and become unstable. Interestingly, in the early stages ($\tau < 6$ h) of the trajectory, the parcel is stable, but its kinetic energy has increased as it encountered falling pressure for $\tau < 3$ h. Only after hour 10, when the parcel has moved more than 200 km to the east, does its kinetic energy grow exponentially in a manner similar to the unstable case of Fig. 3. This case is nonlinear because it depends on the initial location and on the amplitude and direction of the initial velocity perturbation. For example, if the parcel's initial speed is reduced to 10 m s^{-1}; it travels only 135 km to the east in a stable oscillation taking the shape of a cycloid along the y axis.

4. Symmetric instabilities

a. Base state

Consider a dry, ideal gas in hydrostatic and geostrophic balance on an f plane. The temperature is again given by (3.1) but with $\beta = \gamma = 0$. The surface pressure is taken to be a constant given by p_{00}. Because this environment is hydrostatic, one finds

$$p_e(x, z) = p_{00}\left(\frac{T_e}{T_*}\right)^{g/R\Gamma}, \tag{4.1}$$

where

$$T_*(x) = T_0 + \alpha x \tag{4.2}$$

is the surface temperature. The potential temperature of this dry environment is

$$\theta_e = T_e\left(\frac{p_{00}}{p_e}\right)^{R/c_p} = T_*\left(\frac{T_e}{T_*}\right)^{[1-(g/c_p\Gamma)]}, \tag{4.3}$$

and the density field is

$$\rho_e = \rho_*\left(\frac{T_e}{T_*}\right)^{[(g/R\Gamma)-1]}, \tag{4.4}$$

where the surface density is

$$\rho_* = \frac{p_{00}}{RT_*}. \tag{4.5}$$

The longitudinal geostrophic wind is described by

$$f v_e = \frac{1}{\rho_e}\frac{\partial p_e}{\partial x} = g\frac{\alpha}{\Gamma}\left(1 - \frac{T_e}{T_*}\right) \tag{4.6}$$

that vanishes at the surface $z = 0$ and increases with height and has anticyclonic shear with the gradients

$$\frac{\partial v_e}{\partial x} = -\frac{\alpha v_e}{T_*}, \qquad \frac{\partial v_e}{\partial z} = \frac{\alpha g}{f T_*} \tag{4.7}$$

for $\alpha > 0$.

b. Parcel dynamics

Invoking parcel theory, it is assumed that the pressure of the parcel is equal to the pressure of the environment, $p_p = p_e$. The Lagrangian equations of motion for a parcel are

$$\frac{\partial u_p}{\partial \tau} = -\frac{1}{\rho_p}\frac{\partial p_e}{\partial x} + f v_p = f\left(v_p - \frac{\rho_e}{\rho_p} v_e\right), \tag{4.8a}$$

$$\frac{\partial v_p}{\partial \tau} = -f u_p, \tag{4.8b}$$

$$\frac{\partial w_p}{\partial \tau} = -\frac{1}{\rho_p}\frac{\partial p_e}{\partial z} - g = g\left(\frac{\rho_e - \rho_p}{\rho_p}\right), \tag{4.8c}$$

$$\frac{\partial \theta_p}{\partial \tau} = 0, \tag{4.8d}$$

$$\frac{\partial x_p}{\partial \tau} = u_p, \qquad \frac{\partial z_p}{\partial \tau} = w_p. \tag{4.8e}$$

This nonlinear set of coupled equations is solved numerically using a Runge–Kutta technique. The algorithm involves the diagnosis of the density of the parcel ρ_p given its pressure and potential temperature θ_p. For a dry parcel, ρ_p may be determined analytically from the standard expression. For a moist parcel, θ_p is the equivalent potential temperature of the parcel, and the density is determined iteratively using the numerical procedure given in Tripoli and Cotton (1981).

c. Three cases of symmetric instability

We assume inviscid, adiabatic, parcel dynamics and examine the parcel's motion and available energetics in three different environmental flows corresponding to nonhydrostatic, hydrostatic, and conditional symmetric instability. The first two cases represent an extension to a compressible fluid of the Boussinesq results of Emanuel (1983a). The parcel initially lies at the origin and, at the initial time, is given a velocity perturbation.

It is noted from the outset the a posteriori result that the parcel's density varies only slightly from that of the environment. Specifically the density difference is less than or equal to 6×10^{-4}, 2×10^{-4}, and 6×10^{-3} kg m^{-3} in the nonhydrostatic, hydrostatic, and conditional results. As a result, the transverse momentum equation (4.8a) may be accurately approximated by (3.7) using the pseudoabsolute momenta.

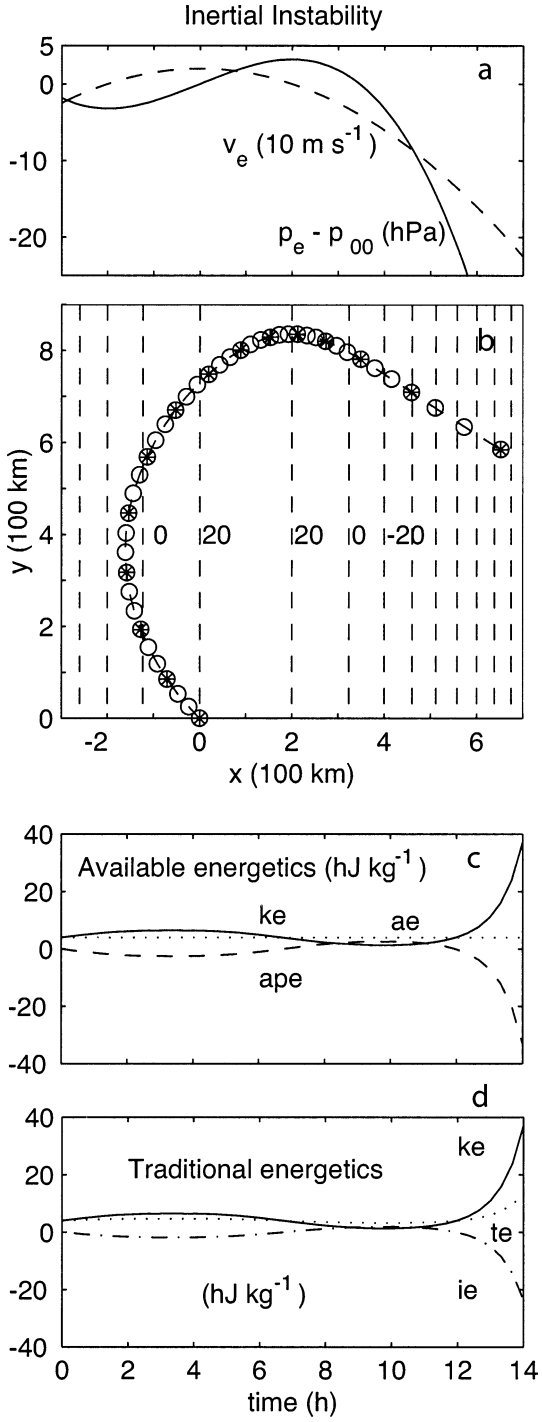

FIG. 5. As in Fig. 2, but for the case of an unstable longitudinal jet.

For the case of nonhydrostatic, symmetric instability, the lapse rate is adiabatic $\Gamma = g/c_p$ and the transverse temperature gradient α is 40°C (1000 km)$^{-1}$. Then the M and θ surfaces of the environment are nearly horizontal and vertical lines (Fig. 6a). Because the slope of the θ surface is larger than that of the M surfaces, Boussinesq theory (Emanuel 1983a) predicts an unstable flow. For the initial velocity perturbation of $(u_i, w_i) = (-1, 1)$ m s^{-1}, the parcel trajectory (Fig. 6a) in the transverse plane is a straight line at an angle of 45° and agrees well with the theoretical trajectories (Emanuel 1983a)

$$x_p = -u_0 \sinh \sigma\tau, \qquad z_p = u_0 \sinh \sigma\tau, \tag{4.9}$$

where $u_0 = 1$ m s^{-1} and $\sigma = (f\partial v_e/\partial z)^{1/2} = 1.16\ 10^{-3}$ s^{-1}. Quantitatively, the velocity field after 45 min is $(u, v, w) = (-11.5, 1.0, 11.5)$ m s^{-1} and is within 1% of theory. It is straightforward to show that, because the horizontal variation in the temperature is small, the parcel equations (4.8a) and (4.8c) reduce to (9) and (10) of Emanuel (1983a).

The available energetics (Fig. 6b) indicates that the kinetic energy of the perturbation grows at the expense of the available potential energy that is the change in the parcel's dry static energy $c_pT + gz$. Mathematically one finds

$$\frac{\partial \text{ke}}{\partial \tau} = \frac{\partial}{\partial \tau}\left(\frac{u_p^2 + v_p^2 + w_p^2}{2}\right)$$

$$= -\frac{u_p}{\rho_p}\frac{\partial p_e}{\partial x} + w_p g\left(\frac{\rho_e - \rho_p}{\rho_p}\right) = -\frac{\partial \text{ape}}{\partial \tau}. \tag{4.10}$$

Although the potential energy of the parcel is increasing with time, the decreasing enthalpy more than compensates, and the available potential energy is negative. This behavior indicates that the rate of cooling of the parcel is greater than the dry adiabatic lapse rate $g/c_p = 9.8$°C km^{-1}. In this case, the parcel has cooled 96.7°C compared to the adiabatic 96.5°C over the ascent of 9.9 km.

Symmetric available potential energy (SAPE) is defined as

$$\text{SAPE} \equiv \int_{\tau_i}^{\tau_f}\left[-\frac{u_p}{\rho_p}\frac{\partial p_e}{\partial x} + w_p g\left(\frac{\rho_e - \rho_p}{\rho_p}\right)\right] d\tau$$

$$= \text{ape}(\tau_i) - \text{ape}(\tau_f), \tag{4.11}$$

as the change in the kinetic energy due to the work done by the horizontal pressure gradient force and the buoyancy from some initial to some final time following the parcel. The second equality follows from the second equality in (4.10) and states that the SAPE is just the difference in the parcel's static energy at the two times. In addition, SAPE = IAPE + CAPE, where the convective available potential energy is the work done by the buoyancy force. In contrast, the slantwise convective available potential energy (Emanuel 1983b) is

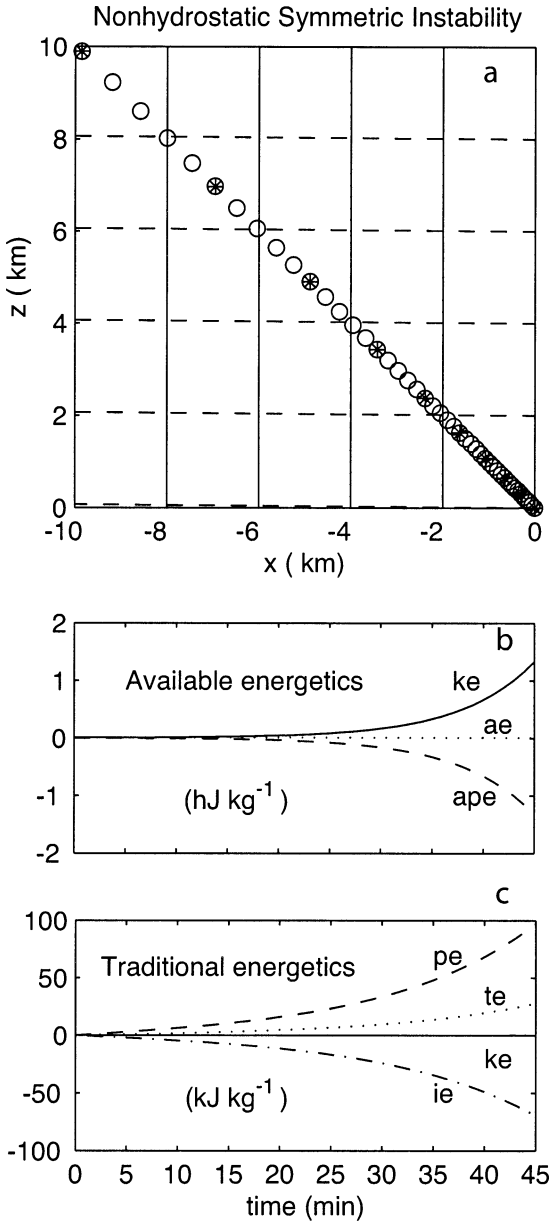

FIG. 6. (a) Parcel trajectory and (b) available and (c) traditional energetics as a function of time for the case of nonhydrostatic symmetric instability. In (a), the parcel location in the transverse plane is indicated with an open circle every minute and with an asterisk every 5 min. The parcel is initially at the origin. The solid and dashed lines in (a) are contours of the potential temperature and pseudoabsolute momentum with contour intervals of 0.08°C and 27 m s^{-1}. At the origin, $\theta_e = 290$ K and $M_e = 0$ m s^{-1}. In (b), the kinetic and available potential energies are indicated as solid and dashed curves. Their sum, the available energy ae indicated by the dotted curve, is a constant. In (c), the kinetic, potential, internal, and total energies are indicated by the solid, dashed, dashed–dotted, and dotted curves.

$$\text{SCAPE} \equiv \int_{\tau_i}^{\tau_f}\left[-\frac{u_p}{\rho_p}\frac{\partial p_e}{\partial x} + fv_p + w_p g\left(\frac{\rho_e - \rho_p}{\rho_p}\right)\right] d\tau, \tag{4.12}$$

and describes the change in the kinetic energy in the transverse plane. Because the parcel conserves its pseudoabsolute momentum, one finds

$$\text{SAPE} = \text{SCAPE} + \frac{f^2(x_f^2 - x_i^2)}{2}. \qquad (4.13)$$

In this case (i.e., Fig. 6), the parcel's transverse displacement is small and the SAPE and SCAPE are approximately the same.

The convenient results (4.11) and (4.13) enable one to diagnose the kinetic energy change of the parcel and its partitioning into transverse and longitudinal contributions from the change in the parcel's static energy and transverse position. The present analysis differs from that of Thorpe et al. (1989, section 3) who divide the flow into mean and eddy components, as well as transverse and longitudinal contributions. Here, (4.11) describes the total change in kinetic energy while the second term on the right-hand side of (4.13) describes the change in the longitudinal component of the kinetic energy. Subtraction of the latter from the former yields the kinetic energy change of the transverse motion (i.e., the SCAPE).

In the traditional energetics (Fig. 6c), the changes in the potential and internal energies dominate that in the kinetic energy. The increase in the parcel's total energy is associated with its increase in potential energy with partial compensation in a decrease in internal energy as it cools during its ascent.

The case of hydrostatic symmetric instability (Fig. 7) produces a large transverse displacement and the differences between SAPE and SCAPE are significant. Here, the lapse rate is stable $\Gamma = 6.5°\text{C km}^{-1}$, and, again, the transverse temperature gradient α is 40°C over 1000 km. The M surfaces are less steeply sloping than the θ surfaces (Fig. 7a), suggesting instability. Initially, the parcel has a velocity of 17.5 m s^{-1} directed along the 290-K θ surface. The trajectory (Fig. 7a) indicates that the parcel stays on this surface. Then the transverse momentum equation (4.8a) reduces to that in terms of the pseudoabsolute momentum (3.7). If the parcel had the same speed but were directed along the M surface, the results would be similar. The energetics (Fig. 7b) indicates that the parcel's kinetic energy increases 28.7 hJ kg^{-1} with most (17.7 hJ kg^{-1}) realized as kinetic energy of the longitudinal wind. In contrast, the SCAPE is 11.0 hJ kg^{-1}. Concomitant with the larger increase in kinetic energy of this case than that of Fig. 6, the parcel has cooled 65.7°C compared to the adiabatic amount of 62.9°C. The energetics (Figs. 7a,b) are qualitatively similar to the nonhydrostatic case of Fig. 6.

The third case of symmetric instability is that of a moist, but initially unsaturated, air parcel in an otherwise dry atmosphere that is stable to dry upright and slantwise convection ($\Gamma = 6.5°\text{C km}^{-1}$ and $\alpha = 2.0\ 10^{-5}$ °C m^{-1}) whose θ surfaces are flatter than the M surfaces (Fig. 8a). Initially, the parcel is at the origin

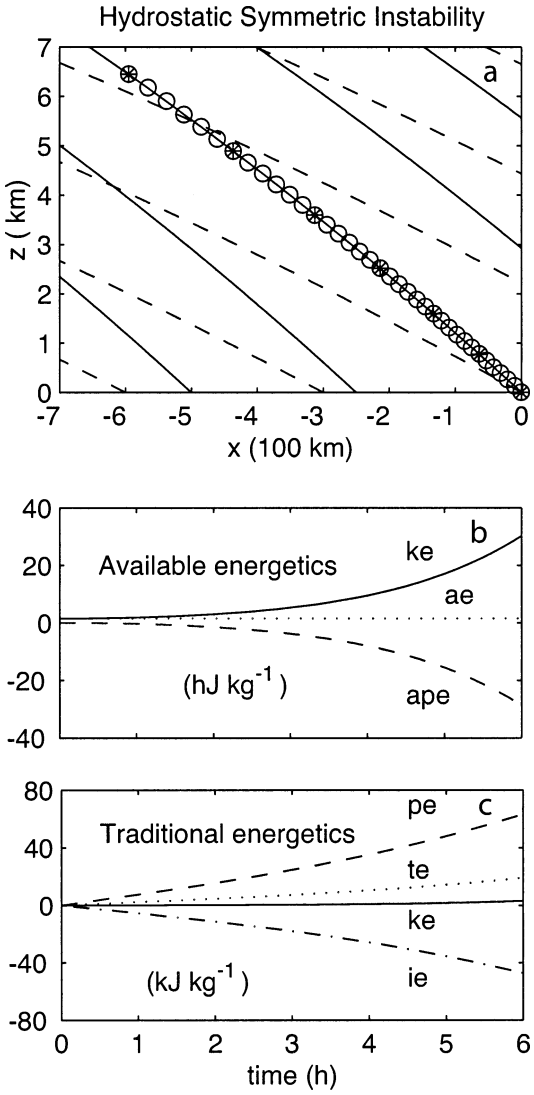

FIG. 7. As in Fig. 6, for the case of hydrostatic symmetric instability. In (a) the parcel location is indicated with an open circle every minute and with an asterisk every 5 min. The solid and dashed lines in (a) are contours of the potential temperature and pseudoabsolute momentum with contour intervals of 10°C and 30 m s^{-1}.

and is neutrally buoyant at a temperature of 288.64 K and a relative humidity of 65%. Then, the parcel is given an initial velocity of 17.5 m s^{-1} along an M surface. The parcel's subsequent trajectory (Fig. 8a) exhibits several interesting features. For the first 2 h, the parcel moves along a constant density surface (approximately the 290 K contour). It undergoes a very weak oscillation about this surface. Inspection of the velocity fields at a resolution (not shown) greater than that in Fig. 8b indicates that the oscillation is a dry buoyancy oscillation. After about 2 h, the parcel has reached its lifting condensation level and rises rapidly. For the next 3 h, it exhibits an oscillatory behavior with an average period of about 15 min as it rises and moves westward.

The energetics (Figs. 8b,c) show that kinetic energy

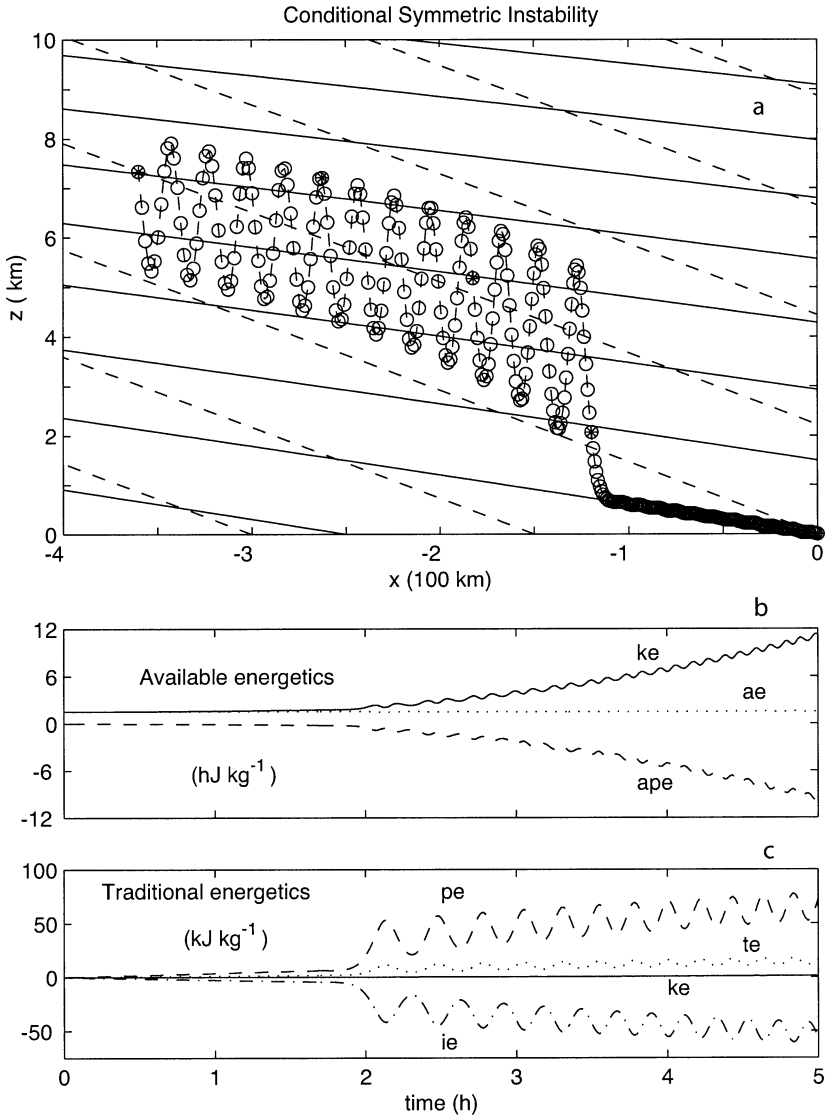

FIG. 8. As in Fig. 7, for the case of conditional symmetric instability. In (a) the parcel location is indicated with an open circle every minute and with an asterisk every 60 min.

is conserved for the first 2 h and then increases as the instability ensues. The oscillation appears in all the energies but the available energy. Over the 5-h period of the integration, the parcel's kinetic energy has increased 9.78 hJ kg^{-1} with most (6.48 hJ kg^{-1}) realized as ke of the longitudinal wind. In contrast, the SCAPE is 3.30 hJ kg^{-1}. The change in the longitudinal wind is consistent with the parcel conserving its pseudoabsolute momentum as it moved 360 km westward.

Figure 9a indicates that the oscillation is primarily contained in the vertical velocity component with only a weak contribution to the transverse wind field. Thus, the oscillation is essentially a buoyancy oscillation. Its period decreases with time as its amplitude increases slightly. The increase in frequency can be attributed to the fact that, as the parcel undergoes its mean ascent, it is cooling on average and the oscillation is gradually transforming itself from a moist to a dry oscillation (Fig. 9b). This behavior is consistent with the decrease in the amplitude of the vertical displacements (Fig. 8a). Recall that the vertical displacement of a parcel undergoing a buoyancy oscillation is inversely proportional to the frequency. The cause of the small increase in the amplitude of the vertical velocity is not clear.

The transverse wind field (Fig. 9a) undergoes a transition once condensation occurs. Before that time the parcel is symmetrically stable, and the parcel is being decelerated transversely (3.7). This decrease in transverse kinetic energy is offset by an increase in the longitudinal kinetic energy and kinetic energy is conserved (Fig. 8b). After the onset of condensation and the vertical jump in the parcel's position, the ambient pseu-

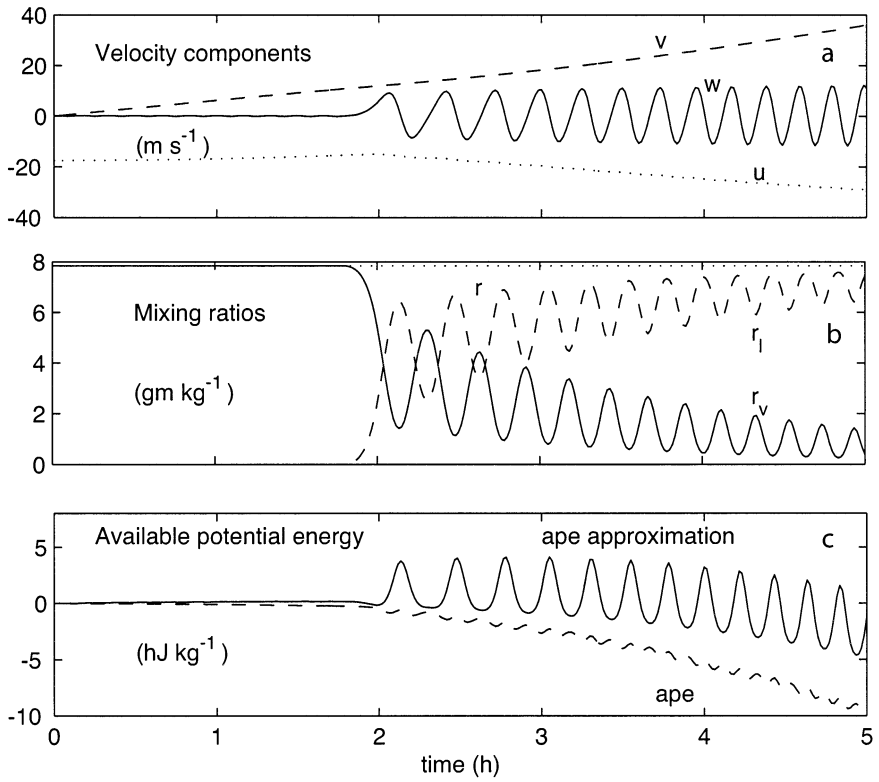

FIG. 9. (a) Velocity components, (b) mixing ratios, and (c) available potential energies as a function of time for the case of Fig. 8. In (a), the dotted, dashed, and solid curves denote the transverse, longitudinal, and vertical velocity components. In (b), the solid, dashed, and dotted curves denote the mixing ratio of water vapor, liquid water, and total water. In (c), the dashed and solid curves are the available potential energy using the exact (4.14) and approximate (4.17) expressions for the enthalpy.

doabsolute momentum M_e increases, and the parcel is symmetrically unstable and is accelerated westward.

In treating this moist case, extra care must be taken to define the enthalpy accurately and conveniently. The enthalpy k per unit mass of cloudy air is

$$(1 + r)k = k_{a0} + rk_{v0} + (c_{pa} + rc_{pv})T - r_l l_v, \quad (4.14)$$

where $k_{\alpha 0}$ and k_{v0} are reference values of the enthalpy for the dry air and water vapor:

$$k_{a0} \equiv k_a(T_{00}) - c_{pa}T_{00}, \quad (4.15a)$$

$$k_{v0} \equiv k_v(T_{00}) - c_{pv}T_{00}, \quad (4.15b)$$

where subscripts a and v denote the dry air and water vapor, and T_{00} is a reference temperature. The mixing ratios of water vapor, liquid water, and total water are r_v, r_l, and r. Here, c_{pa} and c_{pv} are the specific heats at constant pressure for the dry air and water vapor. It is assumed that these specific heats are constants independent of temperature but allow the enthalpy of vaporization l_v to satisfy Kirchhoff's relation $dl_v = -(c_l - c_{pv})dT$, where c_l is the specific heat of the liquid water. In saturated conditions, the saturation vapor pressure e_{sat} is defined as a function of temperature by the Clausius–Clapeyron equation

$$\frac{d \ln e_{\text{sat}}}{dT} = \frac{l_v}{R_v T^2}, \quad (4.16)$$

such that $e_{\text{sat}} = 6.11$ hPa at $T = 273.16$ K. Here, R_v is the gas constant for water vapor.

The formulation (4.14) is compared to the common assumption (e.g., Madden and Robitaille 1970)

$$k \cong c_{pa}T + r_v l_v \quad (4.17)$$

in Fig. 9c. Thus, the approximation (4.17) fails to capture the conservation of the available energy.

It is noted that the reference values (4.15) of the enthalpies of dry air and water vapor need not be specified for the closed parcels treated so far. In each case, for either the dry or moist cases, the available potential energy is defined as the difference in the enthalpies, and the contributions from these reference values cancel. In the case of an open parcel that may lose mass, these values would, in general, have to be specified. In these situations, it is more convenient to describe the energetics solely in terms of the dry air. Figure 10 presents the same case as Fig. 8 but for pseudoadiabatic ascent of the parcel. Differences with the reversible case (Fig. 8) arise when the condensation occurs and the liquid water falls out. As expected by the decrease in density,

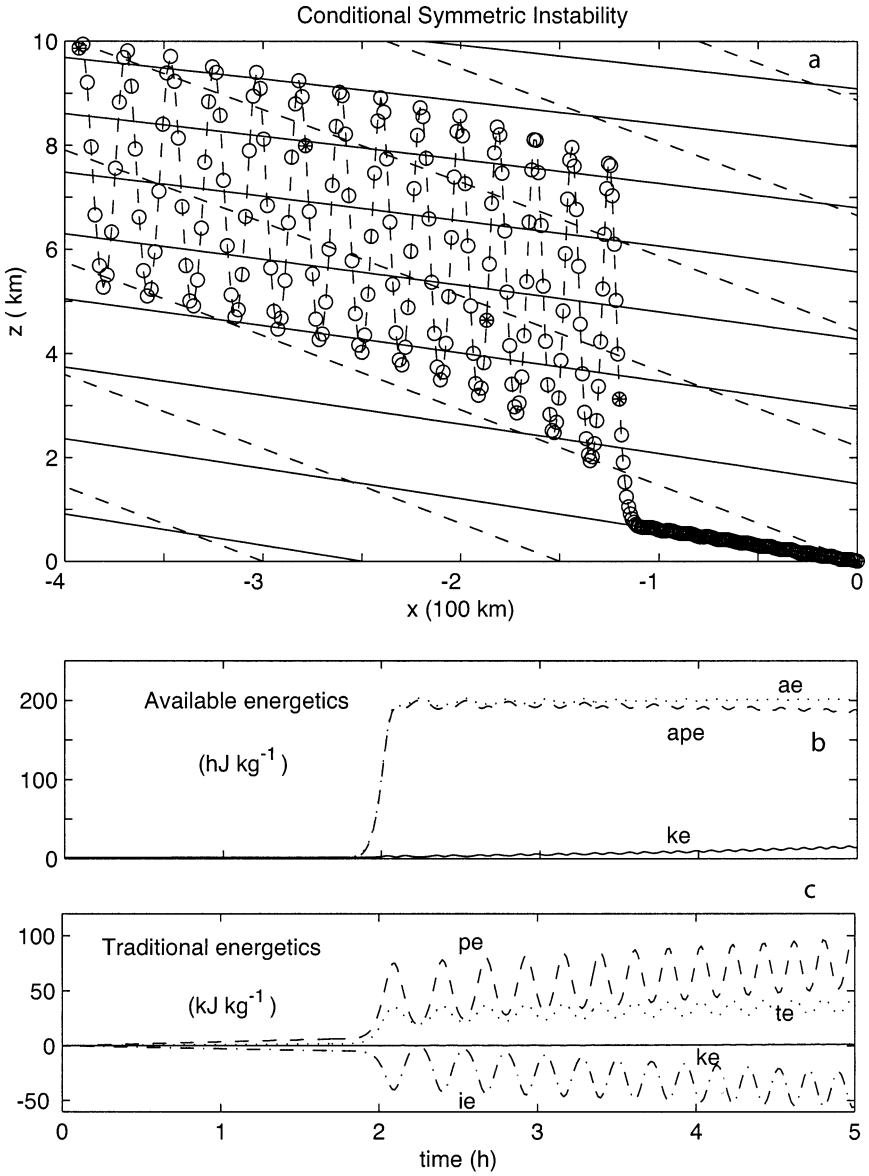

FIG. 10. As in Fig. 8, but for a pseudoadiabatic ascent. Panels (b) and (c) plot the available and traditional energetics for the dry air portion of the parcel. The available energy ae is not conserved.

the amplitude of the oscillation is larger and its period is shortened reflecting a dry buoyancy oscillation.

The available energetics (Fig. 10b) are distinctly different from that of the closed parcel of Fig. 8b. The available energy increases dramatically by 195 hK kg^{-1} near hour 2 due to condensation of most of the parcel's water vapor. (Its original mixing ratio is 7.84 g kg^{-1}.) The parcel's available energy increases slightly at the crest of each subsequent oscillation as additional small amounts of water vapor are condensed out of the parcel. After the fourth hour, the parcel is essentially dry, and its available energy is conserved. The traditional energetics is similar for the reversible (Fig. 8c) and pseudoadiabatic (Fig. 10c) cases with the latter displaying a larger oscillation in the energetics.

5. Conclusions

The major contribution of this investigation is the derivation of the equation for local available energetics (2.10). The derivation (section 2) is simple but general and emphasizes its Lagrangian nature. It extends the derivations of Andrews (1981), Shepherd (1993), and Bannon (2003) for multicomponent flows with nonresting base states.

The utility of the available energetics has been dem-

onstrated for the case of inertial and symmetric instabilities using parcel theory. In this case the parcel's available energy is conserved in adiabatic inviscid flows but not its total energy. The lack of conservation in the latter case is due to the rate of working by the environmental pressure and implies an exchange of energy between the parcel and the environment. For available energetics, the growth of a parcel's kinetic energy occurs at the expense of the available potential energy that becomes negative.

The cases of symmetric instability in section 4 extend the Boussinesq parcel theory of Emanuel (1983a,b) to the compressible case and confirm its validity. The case of conditional symmetric instability displays a convective overshoot and a nonhydrostatic buoyancy oscillation. The SCAPE is related to the available potential energy by (4.13). The SCAPE describes the change in the kinetic energy in the transverse plane and includes a contribution by the Coriolis force. The SAPE describes the change in the total kinetic energy while the second term on the right-hand side of (4.13) describes the change in the longitudinal component of the kinetic energy. All three are independent of the path of the parcel.

Last, it is important to note that the three-dimensional derivation of section 2 is applicable to spherical, f-plane, and β-plane geometries, and that it may be generalized to handle a base state that is changing with time (e.g., Gray and Thorpe 2001). In that case, a term proportional to the local time rate of change of the base-state pressure appears on the right-hand side of (2.5) and (2.7), and (2.10) becomes

$$\frac{\partial \mathrm{ae}}{\partial \tau} = -\frac{1}{\rho_p}\nabla \cdot (p'\mathbf{u}) + \frac{\dot{p}_s}{\rho_p} + \dot{q} + \mathbf{u} \cdot \mathbf{f}, \qquad (5.1)$$

where $\dot{p}_s$ is the base-state pressure tendency.

Acknowledgments. The National Science Foundation, under Grants ATM-9820233 and ATM-0215358, provided partial support for this research. The author benefited from helpful discussions with Jeffrey M. Chagnon on available energetics and with John H. E. Clark on conditional symmetric instability.

REFERENCES

Andrews, D. G., 1981: A note on potential energy density in a stratified compressible fluid. *J. Fluid Mech.,* **107,** 227–236.

Bannon, P. R., 2003: Hamiltonian description of idealized binary geophysical fluids. *J. Atmos. Sci.,* **60,** 2809–2819.

Betts, A. K., and J. F. R. McIlveen, 1969: The energy formula in a moving reference frame. *Quart. J. Roy. Meteor. Soc.,* **95,** 639–642.

Danielsen, E. F., 1961: Trajectories: Isobaric, isentropic and actual. *J. Meteor.,* **18,** 479–486.

Dutton, J. A., 1995: *Dynamics of Atmospheric Motion.* Dover, 617 pp.

Emanuel, K. A., 1983a: The Lagrangian parcel dynamics of moist symmetric instability. *J. Atmos. Sci.,* **40,** 2368–2376.

——, 1983b: On assessing local conditional symmetric instability from atmospheric soundings. *Mon. Wea. Rev.,* **111,** 2016–2033.

Gray, S. L., and A. J. Thorpe, 2000: Potential energy for slantwise parcel motion. *Atmos. Sci. Lett.,* **1,** doi:10.1006/asle.2000.0006. [Available online at http://www3.interscience.wiley.com/cgi-bin/jissue/107638738.]

——, and ——, 2001: Potential theory in three dimensions and the calculation of SCAPE. *Mon. Wea. Rev.,* **129,** 1656–1672.

Green, J. S. A., F. H. Ludlam, and J. F. R. McIlveen, 1966: Isentropic relative-flow analysis and the parcel theory. *Quart. J. Roy. Meteor. Soc.,* **92,** 210–219.

Holton, J. R., 1992: *An Introduction to Dynamic Meteorology.* 3d ed. Academic Press, 511 pp.

Lorenz, E. N., 1955: Available potential energy and the maintenance of the general circulation. *Tellus,* **7,** 157–167.

Madden, R. A., and F. E. Robitaille, 1970: A comparison of the equivalent potential temperature and the static energy. *J. Atmos. Sci.,* **27,** 327–329.

Margules, M., 1905: On the energy of storms. *Smithson. Misc. Collect.,* **51,** 533–595.

Peslin, M., 1868: Sur les mouvements generaux de 1'atmosphere. *Bull. Hebd. L'Ass. Sci. France,* **3,** 299–319. [See Kutzbach, G., 1979: *The Thermal Theory of Cyclones.* Amer. Meteor. Soc., 85–86, for a summary in English.]

Rauber, R. M., M. K. Ramamurthy, and A. Tokay, 1994: Synoptic and mesoscale structure of a severe freezing rain event: The St. Valentine's Day ice storm. *Wea. Forecasting,* **9,** 183–208.

Shepherd, T. G., 1993: A unified theory of available potential energy. *Atmos.–Ocean,* **31,** 1–26.

Thorpe, A. J., B. J. Hoskins, and V. Innocentini, 1989: The parcel method in baroclinic atmosphere. *J. Atmos. Sci.,* **46,** 1274–1284.

Tripoli, G. J., and W. R. Cotton, 1981: The use of liquid-water potential temperature as a thermodynamic variable in deep atmospheric models. *Mon. Wea. Rev.,* **109,** 1094–1102.

van Mieghem, J. M., 1951: Hydrodynamic instability. *Compendium of Meteorology,* T. F. Malone, Ed., Amer. Meteor. Soc., 434–453.